Atmospheric Chemistry and Physics

Supporting Information for

Modulation of the Intraseasonal Variability of Early Summer Precipitation in Eastern China

by the Quasi-Biennial Oscillation and the Madden-Julian Oscillation

Zefan Ju[1], Jian Rao[1*], Yue Wang[1], Junfeng Yang[2], and Qian Lu[1]

[1]Collaborative Innovation Center on Forecast and Evaluation of Meteorological Disasters / Key Laboratory of Meteorological Disaster of Ministry of Education, Nanjing University of Information Science and Technology, Nanjing 210044, China
[2]National Space Science Center, Chinese Academy of Sciences, Beijing 100190, China

Correspondence to: Dr. Jian Rao (raojian@nuist.edu.cn)
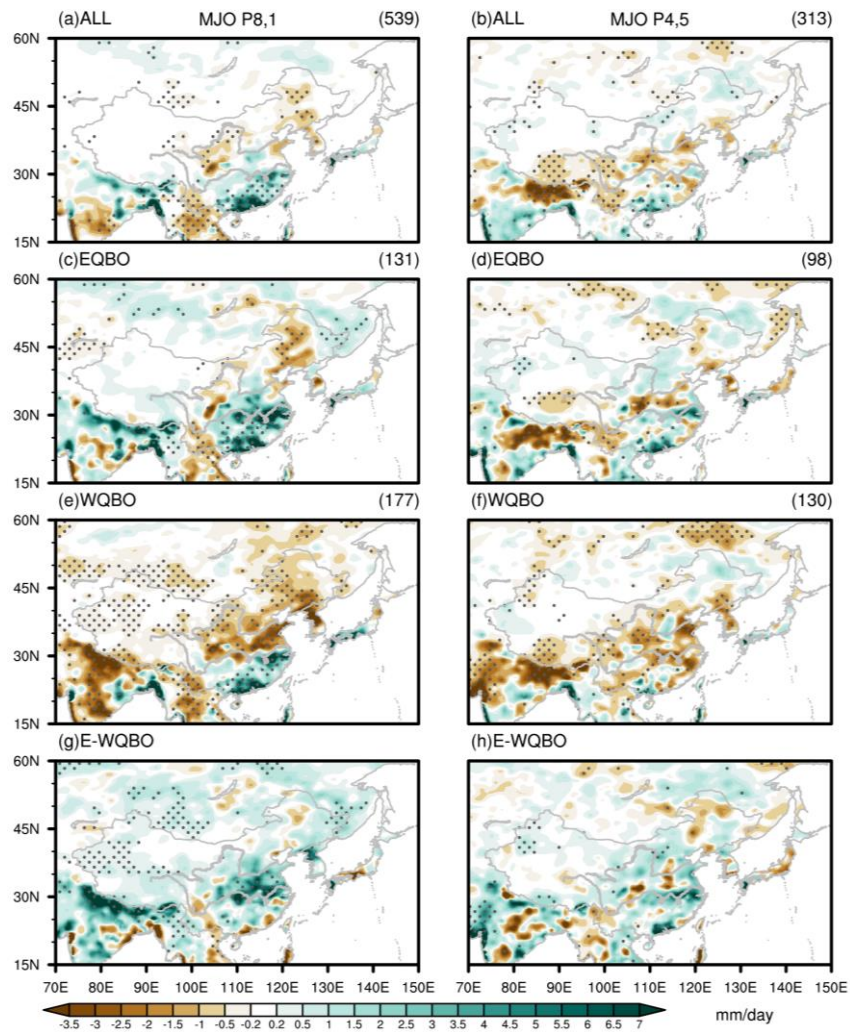
Contents of this file

Figure S1. Composite rainfall anomalies (shadings; units: mm/day) at the MJO phases (left) 8-1 and (right) phases 4-5 for (a, b) total days, (c, d) easterly QBO days, (e, f) westerly QBO days and (g, h) EQBO-WQBO difference after the interannual ENSO signals are removed. The dots denote the composite anomalies at 95% confidence level according to the t-test. The number of days used for each composite group is printed at the top-right corner.
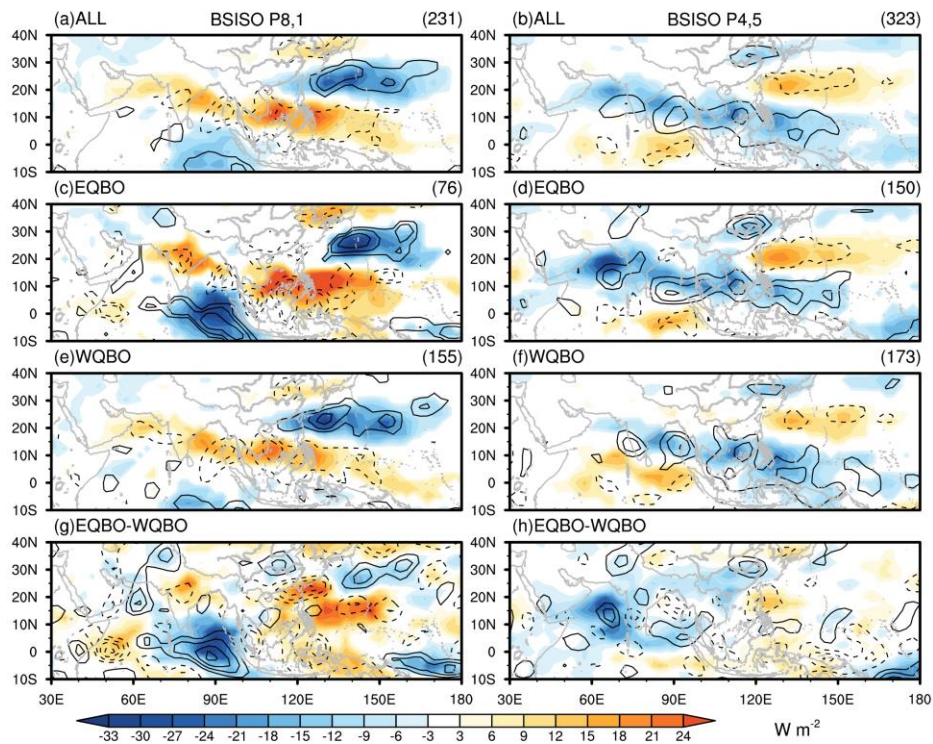
Figure S2. Composite OLR (shadings; units: W/m^2) and 200-hPa divergence (contours; units: s^{-1}; interval: 3×10^{-6}) anomalies at the BSISO1 phases (left) 8-1 and (right) phases 4-5 for (a, b) total days, (c, d) easterly QBO days, (e, f) westerly QBO days and (g, h) EQBO-WQBO difference (dashed lines show convergence anomalies). Only the composite anomalies that are statistically significant at 95% confidence level are shown according to the t-test. The number of days used for each composite map is printed at the top-right corner.
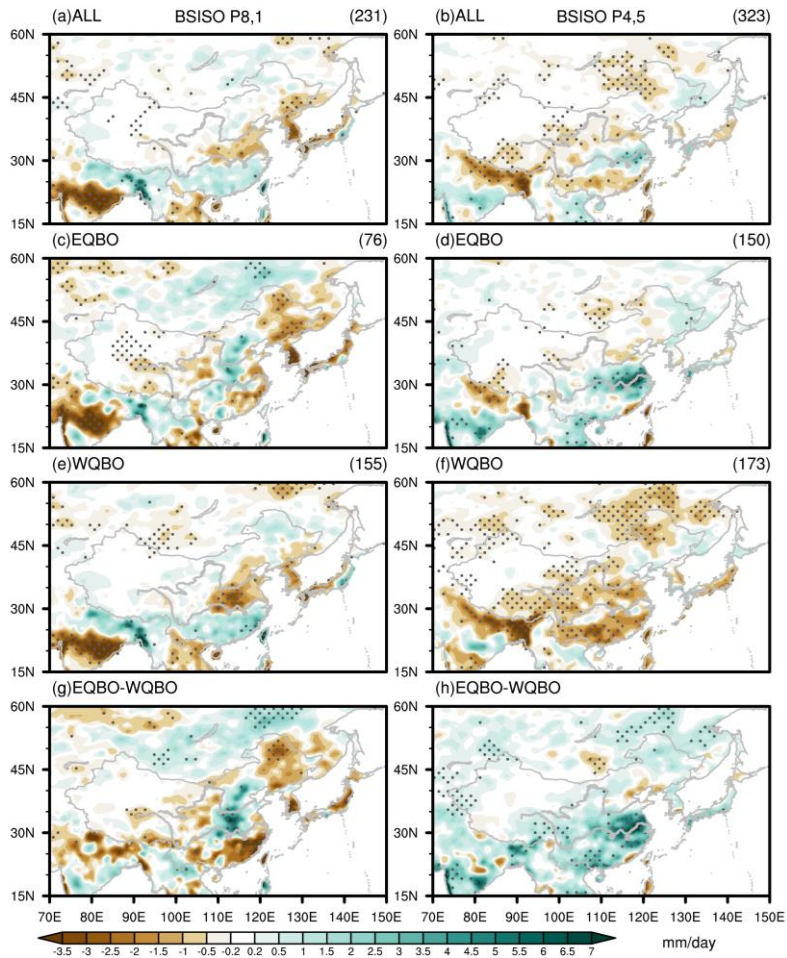
Figure S3. Composite rainfall anomalies (shadings; units: mm/day) at the BSISO1 phases (left) 8-1 and (right) phases 4-5 for (a, b) total days, (c, d) easterly QBO days, (e, f) westerly QBO days and (g, h) EQBO-WQBO difference. The dots denote the composite anomalies at 95% confidence level according to the t-test. The number of days used for each composite map is printed at the top-right corner.
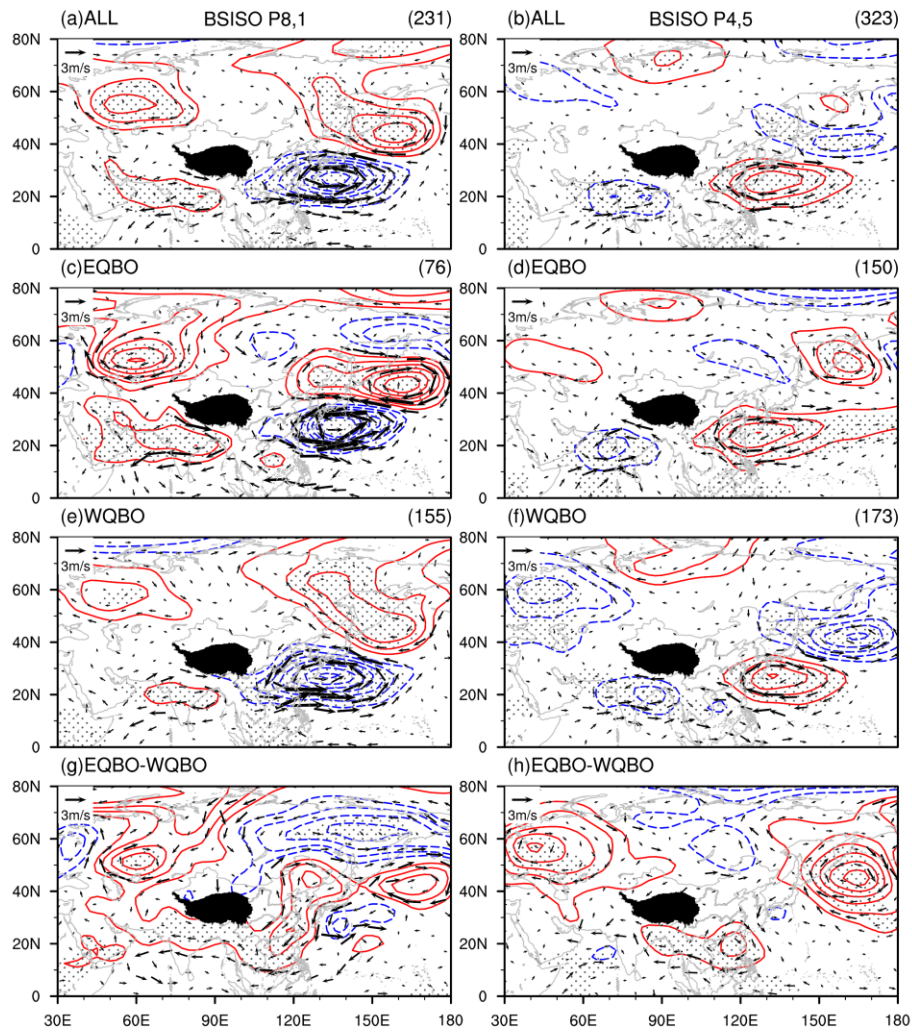
Figure S4. Composite horizontal wind (vectors; units: m/s) and geopotential height (contours; units: gpm; interval: 5) anomalies at 850 hPa during the BSISO1 phases (left) 8-1 and (right) phases 4-5 for (a, b) total days, (c, d) easterly QBO days, (e, f) westerly QBO days and (g, h) EQBO-WQBO difference. Note that zero contours are omitted, the positive contours are shown in red, and the negative contours are shown in blue. The dots denote the composite height anomalies at 95% confidence level according to the t-test. The number of days used for each composite map is printed at the top-right corner.
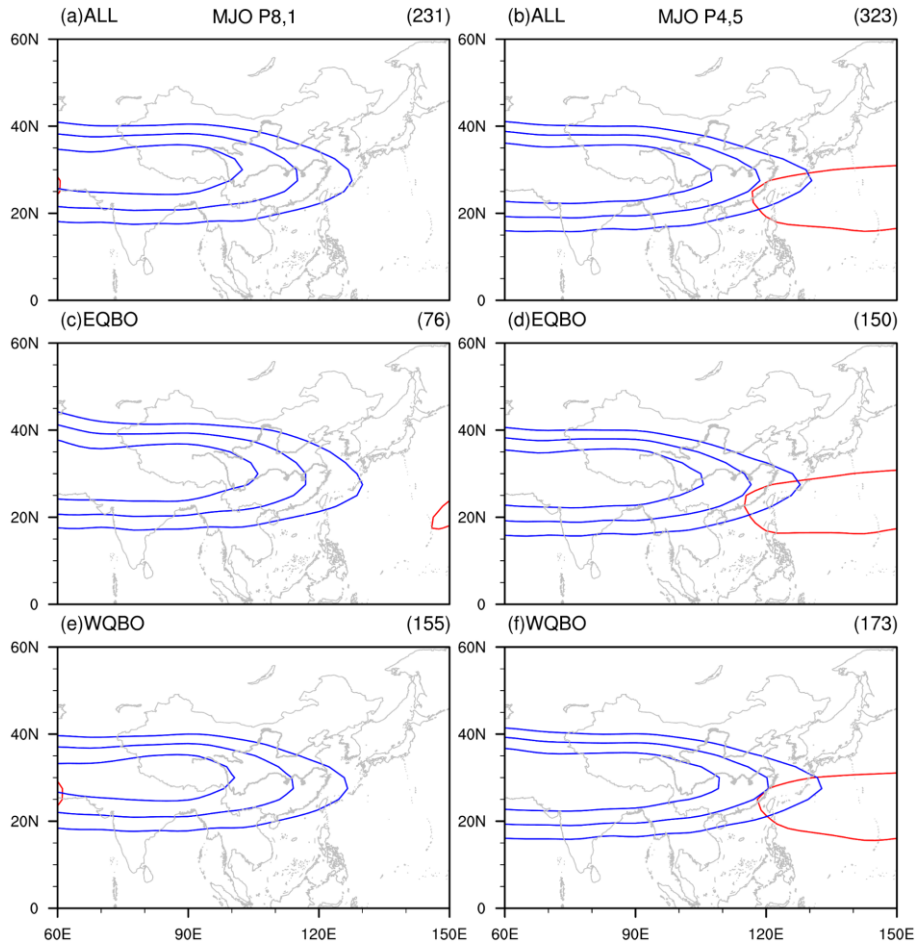
Figure S5. Composited South Asia High (SAH) at 100 hPa and western Pacific high (WPH) at 500 hPa during the BSISO1 phases (left) 8-1 and (right) phases 4-5 for (a, b) total days, (c, d) easterly QBO days, and (e, f) westerly QBO days. Three height contours (16720, 16760, 16800 gpm) are plotted for the SAH, and one contour (5880 gpm) is plotted for the WPSH.
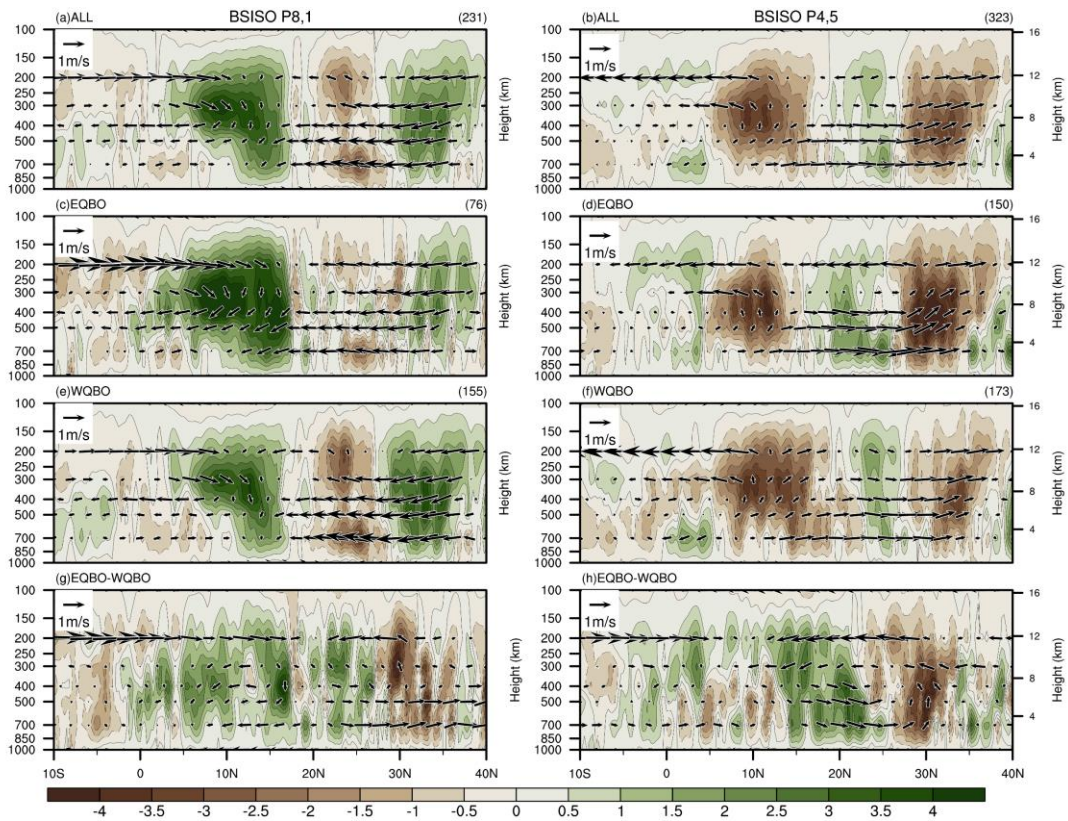
Figure S6. Composited latitude-pressure cross section of meridional circulation anomalies (vectors; units: m/s, Pa/s) and vertical velocity anomalies (shadings; units: 0.01 Pa/s) averaged from 110–120°E during the BSISO1 phases (left) 8-1 and (right) phases 4-5 for (a, b) total days, (c, d) easterly QBO days, (e, f) westerly QBO days and (g, h) EQBO-WQBO difference (brown is upward motion). The vertical velocity anomalies have been multiplied by -10 to better show the vectors.
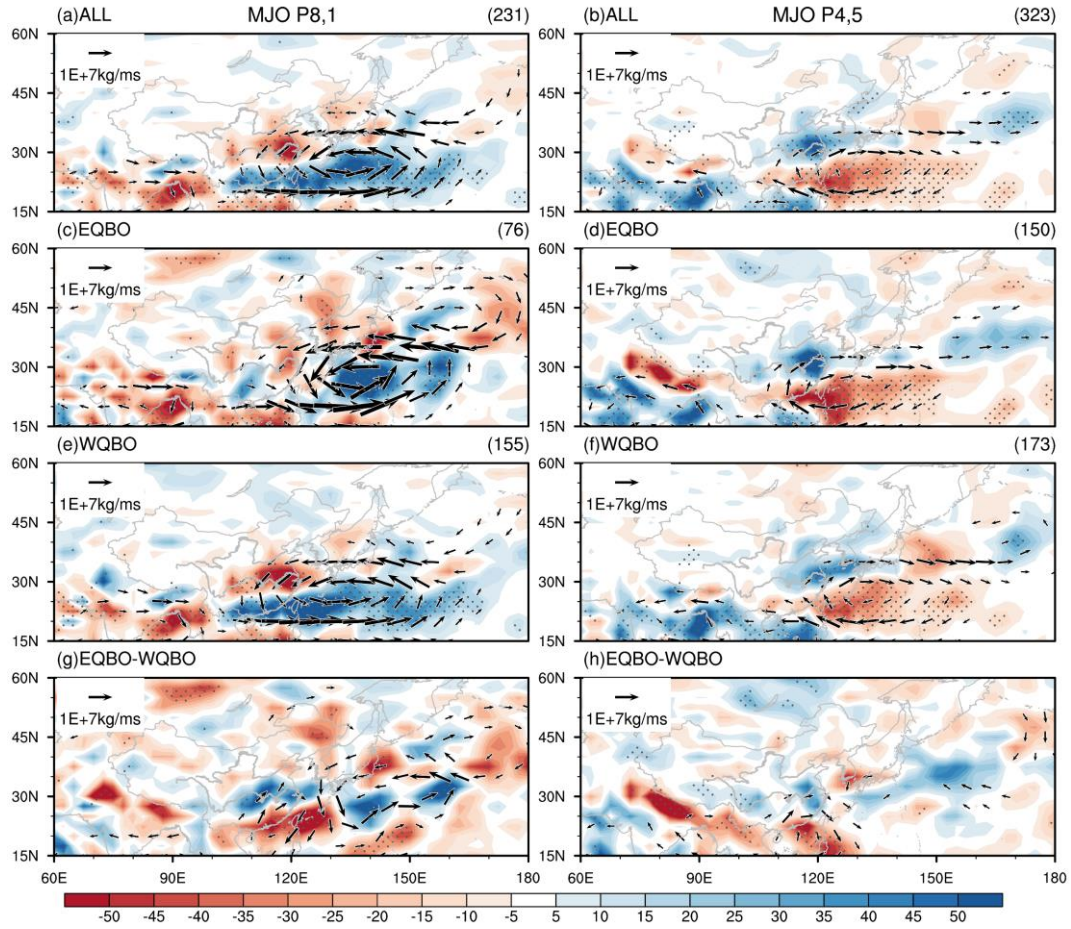
Figure S7. Composited vertically integrated moisture flux (VIMF) anomalies (vectors; units: 10^7 kg m^{-1} s^{-1}) and their horizonal convergence (VIMFC) anomalies (shadings; units: kg m^{-2} s^{-1}) during the BSISO1 phases (left) 8-1 and (right) phases 4-5 for (a, b) total days, (c, d) easterly QBO days, (e, f) westerly QBO days and (g, h) EQBO-WQBO difference. Note that only the VIMF anomalies lager than 0.5×10^7 kg m^{-1}s^{-1} are shown. The VIMFC anomalies that are statistically significant at the 95% confidence level are dotted.
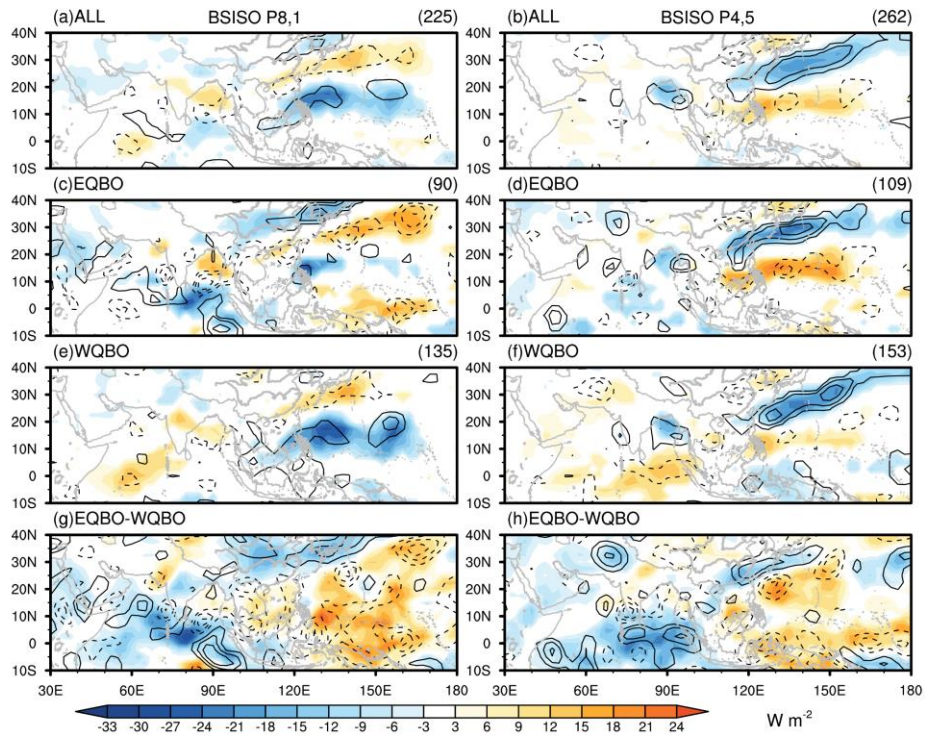
Figure S8. Composite OLR (shadings; units: W/m^2) and 200-hPa divergence (contours; units: s^{-1}; interval: 3×10^{-6}) anomalies at the BSISO2 phases (left) 8-1 and (right) phases 4-5 for (a, b) total days, (c, d) easterly QBO days, (e, f) westerly QBO days and (g, h) EQBO-WQBO difference (dashed lines show convergence anomalies). Only the composite anomalies that are statistically significant at 95% confidence level are shown according to the t-test. The number of days used for each composite map is printed at the top-right corner.
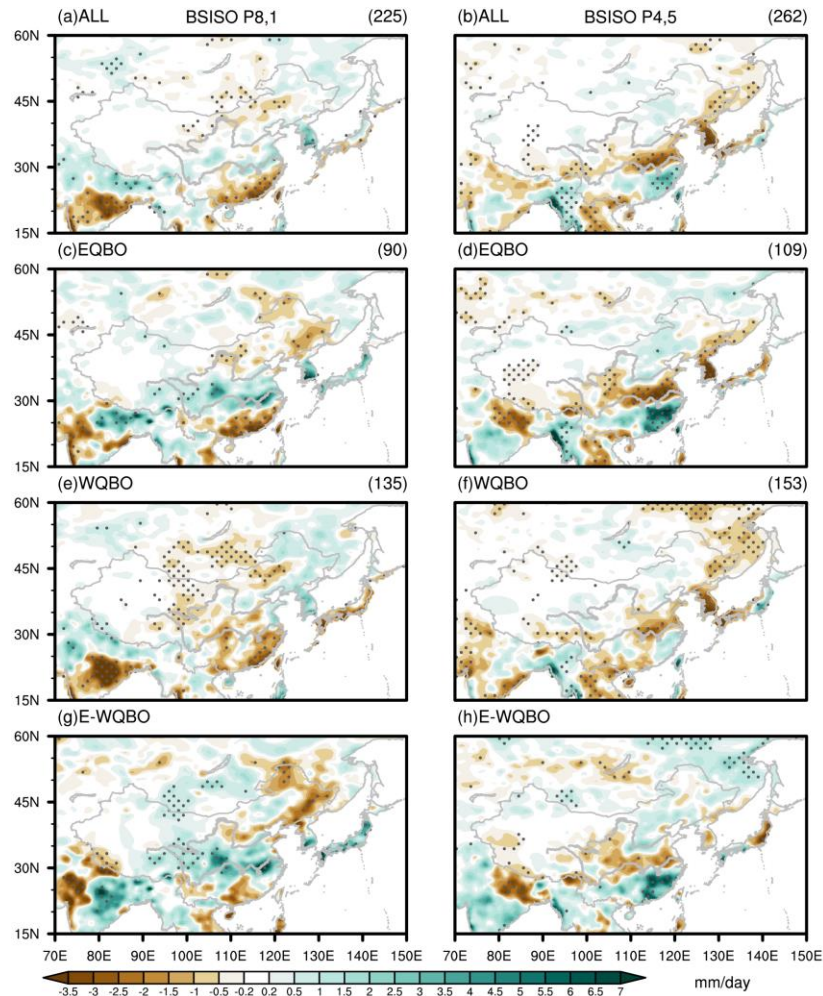
Figure S9. Composite rainfall anomalies (shadings; units: mm/day) at the BSISO2 phases (left) 8-1 and (right) phases 4-5 for (a, b) total days, (c, d) easterly QBO days, (e, f) westerly QBO days and (g, h) EQBO-WQBO difference. The dots denote the composite anomalies at the 95% confidence level according to the t-test. The number of days used for each composite map is printed at the top-right corner.
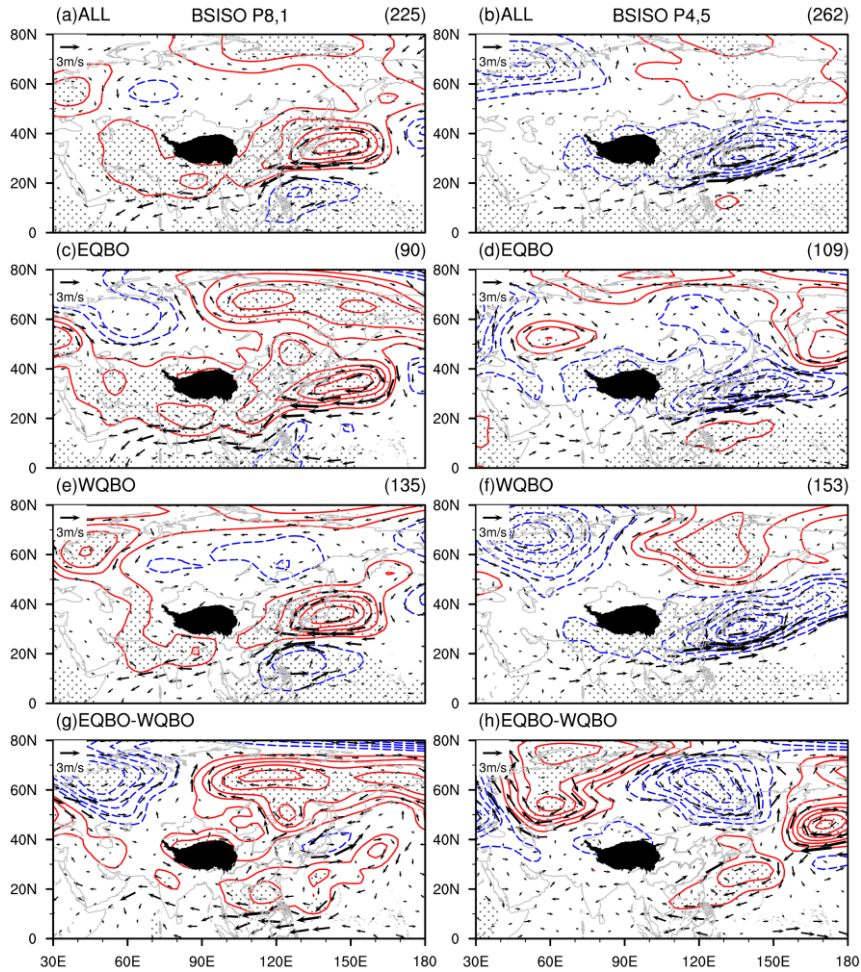
Figure S10. Composite horizontal wind (vectors; units: m/s) and geopotential height (contours; units: gpm; interval: 5) anomalies at 850 hPa during the BSISO2 phases (left) 8-1 and (right) phases 4-5 for (a, b) total days, (c, d) easterly QBO days, (e, f) westerly QBO days and (g, h) EQBO-WQBO difference. Note that zero contours are omitted, the positive contours are shown in red, and the negative contours are shown in blue. The dots denote the composite height anomalies at 95% confidence level according to the t-test. The number of days used for each composite map is printed at the top-right corner.
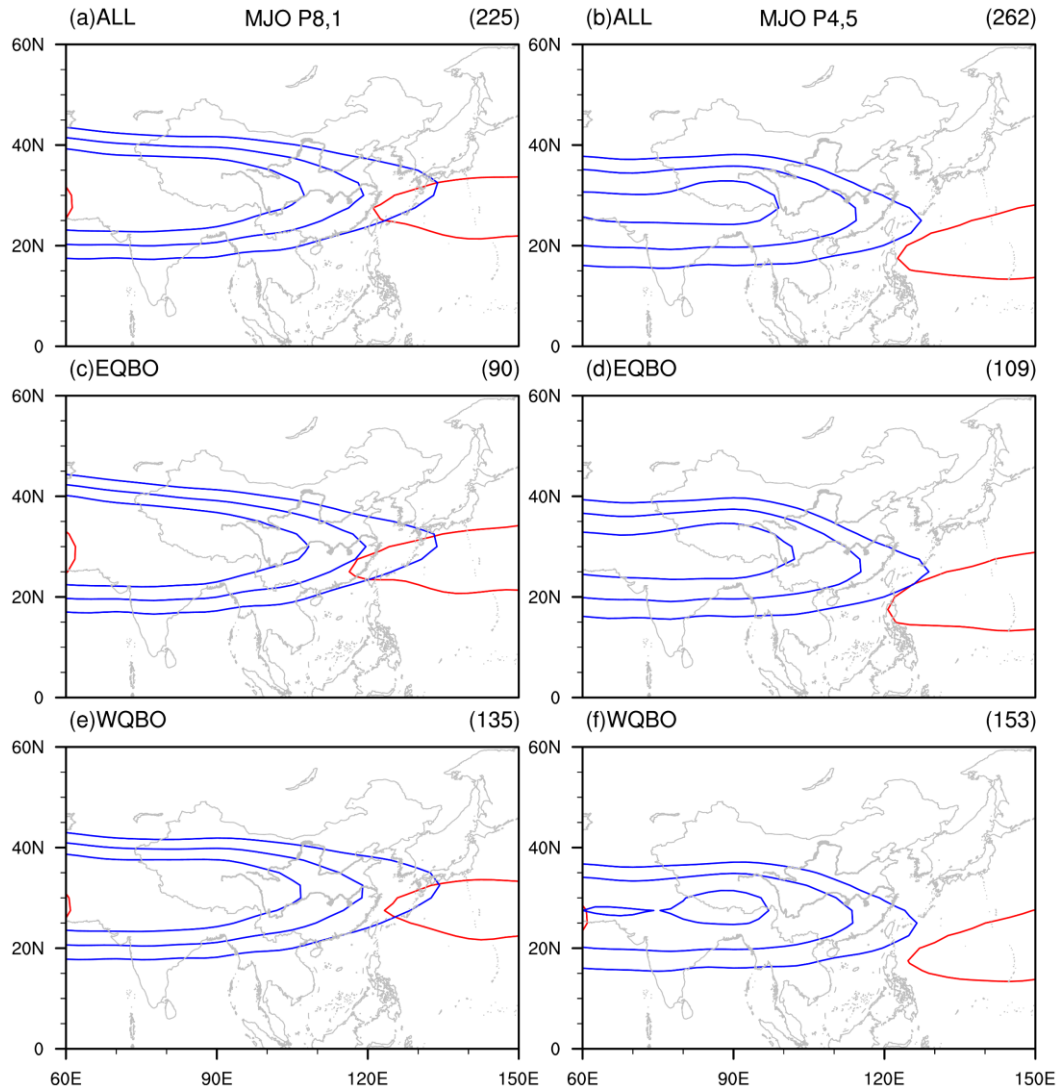
Figure S11. Composited South Asia High (SAH) at 100 hPa and western Pacific high (WPH) at 500 hPa during the BSISO2 phases (left) 8-1 and (right) phases 4-5 for (a, b) total days, (c, d) easterly QBO days, and (e, f) westerly QBO days. Three height contours (16720, 16760, 16800 gpm) are plotted for the SAH, and one contour (5880 gpm) is plotted for the WPSH.
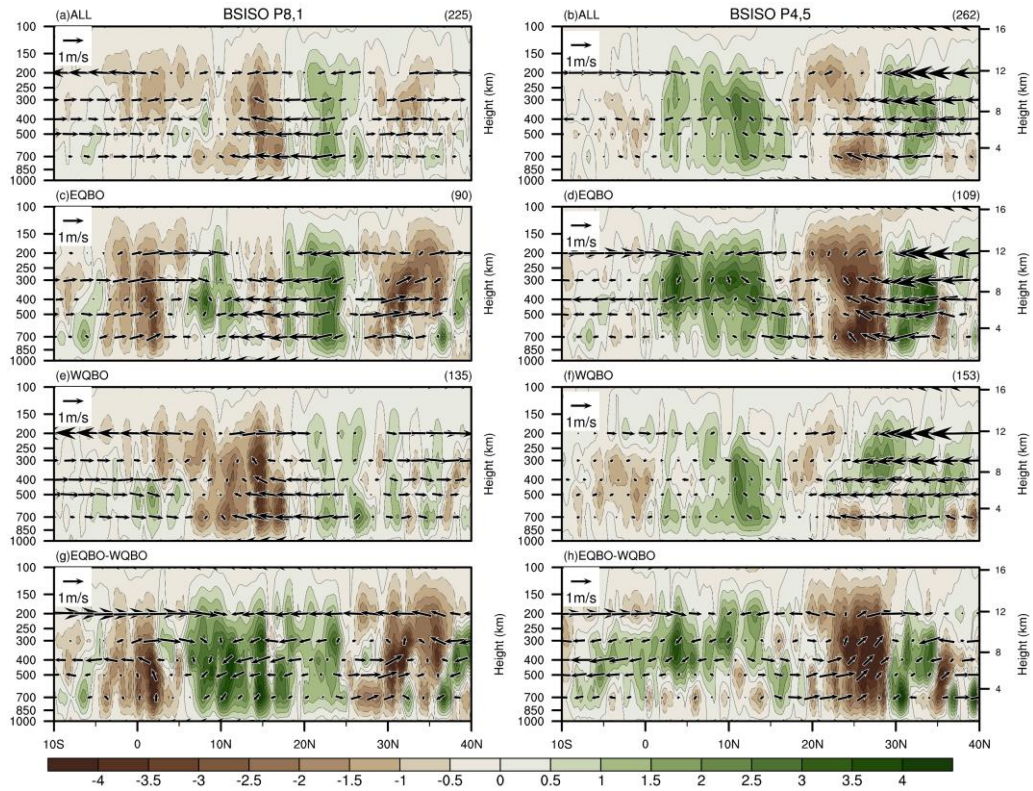
Figure S12. Composited latitude-pressure cross section of meridional circulation anomalies (vectors; units: m/s, Pa/s) and vertical velocity anomalies (shadings; units: 0.01 Pa/s) averaged from 110–120°E during the BSISO2 phases (left) 8-1 and (right) phases 4-5 for (a, b) total days, (c, d) easterly QBO days, (e, f) westerly QBO days and (g, h) EQBO-WQBO difference (brown is upward motion). The vertical velocity anomalies have been multiplied by -10 to better show the vectors.
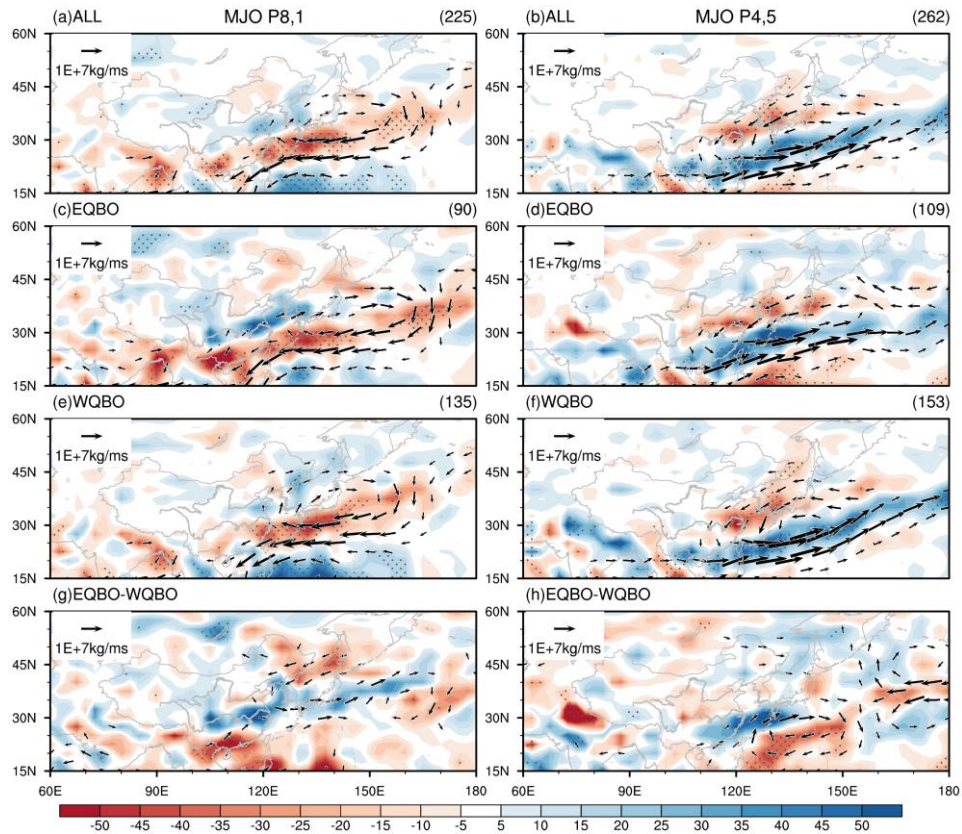
Figure S13. Composited vertically integrated moisture flux (VIMF) anomalies (vectors; units: 10^7 kg m^{-1} s^{-1}) and their horizonal convergence (VIMFC) anomalies (shadings; units: kg m^{-2} s^{-1}) during the BSISO2 phases (left) 8-1 and (right) phases 4-5 for (a, b) total days, (c, d) easterly QBO days, (e, f) westerly QBO days and (g, h) EQBO-WQBO difference. Note that only the VIMF anomalies lager than 0.5×10^7 kg m^{-1}s^{-1} are shown. The VIMFC anomalies that are statistically significant at the 95% confidence level are dotted.
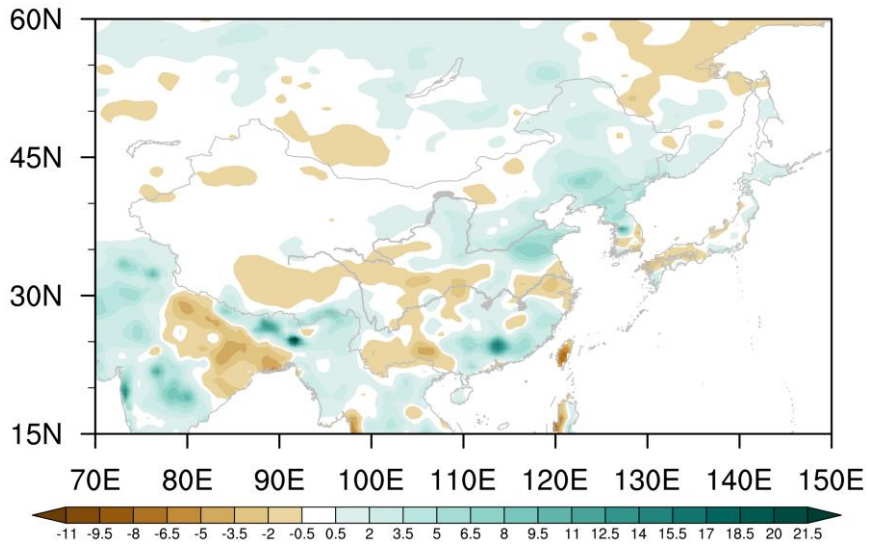
Figure S14. Precipitation anomalies (units: mm/day) during the June-July for 2022.
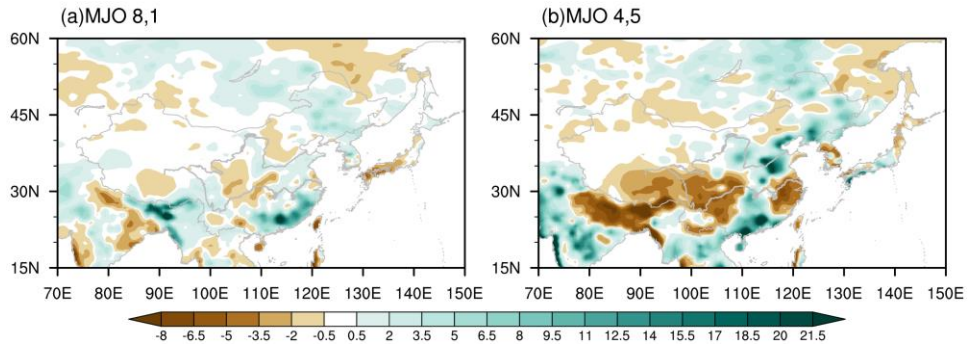
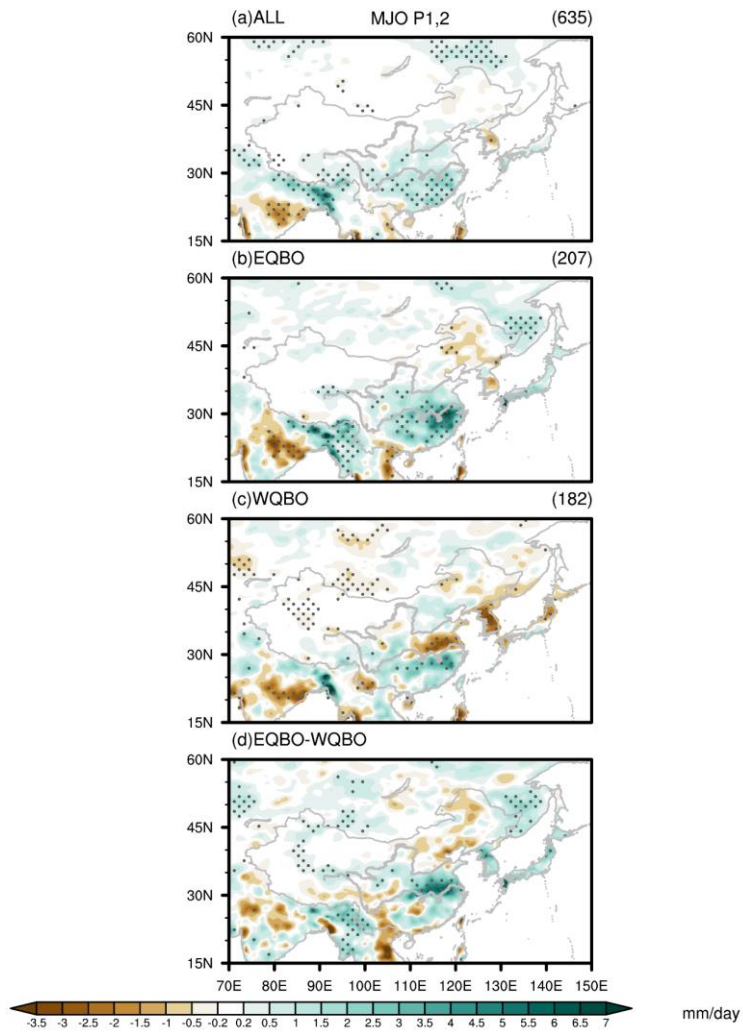**Figure S15. Precipitation anomalies (units: mm/day) during MJO phases (a) 8-1 and (b) 4-5 for 2022.**

Figure S16. Composite rainfall anomalies (shadings; units: mm/day) at the MJO phases 1-2 for (a) total days, (b) easterly QBO days, (c) westerly QBO days and (d) EQBO-WQBO difference. The dots denote the composite anomalies at 95% confidence level according to the t-test. The number of days used for each composite map is printed at the top-right corner.
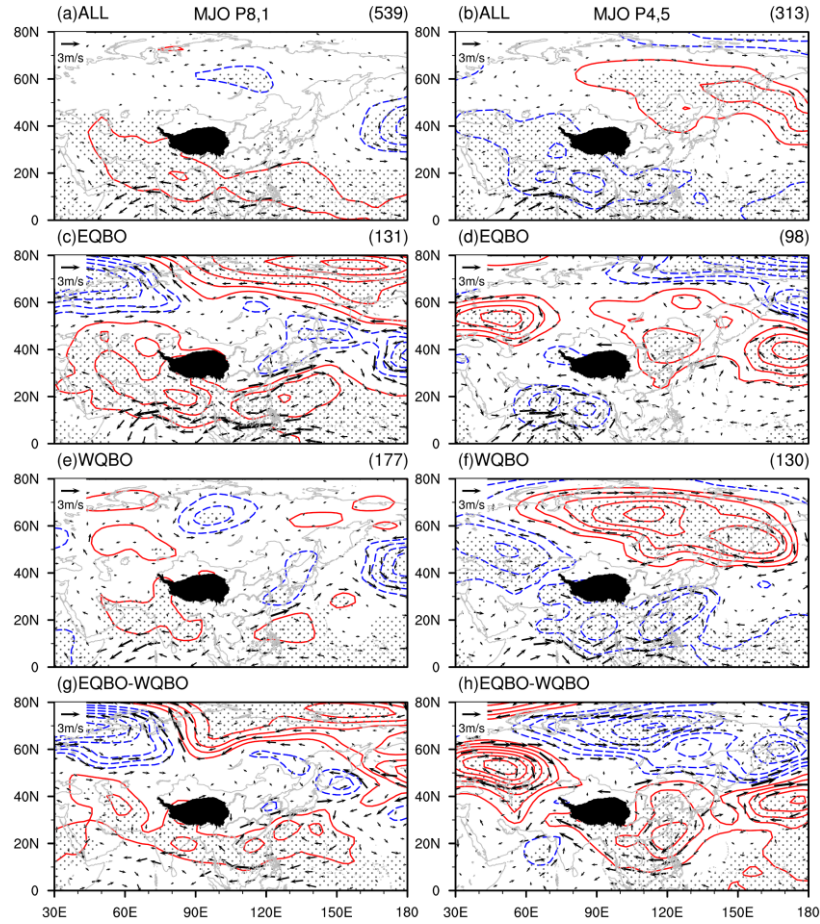
Figure S17. Composite horizontal wind (vectors; units: m/s) and geopotential height (contours; units: gpm; interval: 5) anomalies at 850 hPa using the NCEP-NCAR reanalysis during the MJO phases (left) 8-1 and (right) phases 4-5 for (a, b) total days, (c, d) easterly QBO days, (e, f) westerly QBO days and (g, h) EQBO-WQBO difference. Note that zero contours are omitted, the positive contours are shown in red, and the negative contours are shown in blue. The dots denote the composite height anomalies at 95% confidence level according to the t-test. The number of days used for each composite map is printed at the top-right corner.
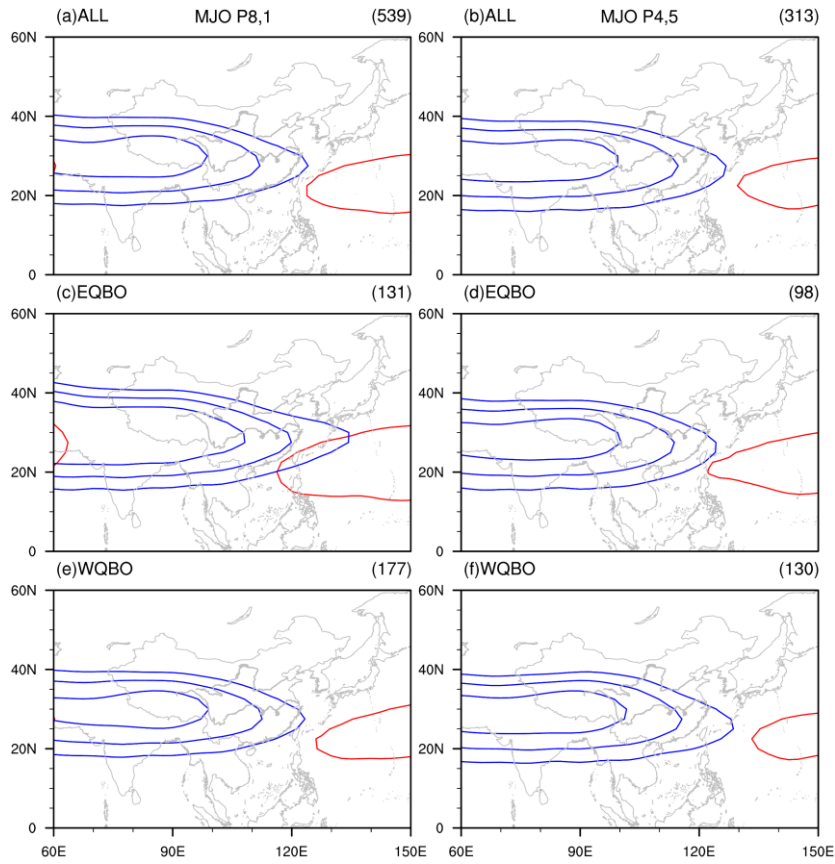
Figure S18. Composited South Asia High (SAH) at 100 hPa and western Pacific high (WPH) at 500 hPa using the NCEP-NCAR reanalysis during the MJO phases (left) 8-1 and (right) phases 4-5 for (a, b) total days, (c, d) easterly QBO days, and (e, f) westerly QBO days. Three height contours (16720, 16760, 16800 gpm) are plotted for the SAH, and one contour (5880 gpm) is plotted for the WPSH.
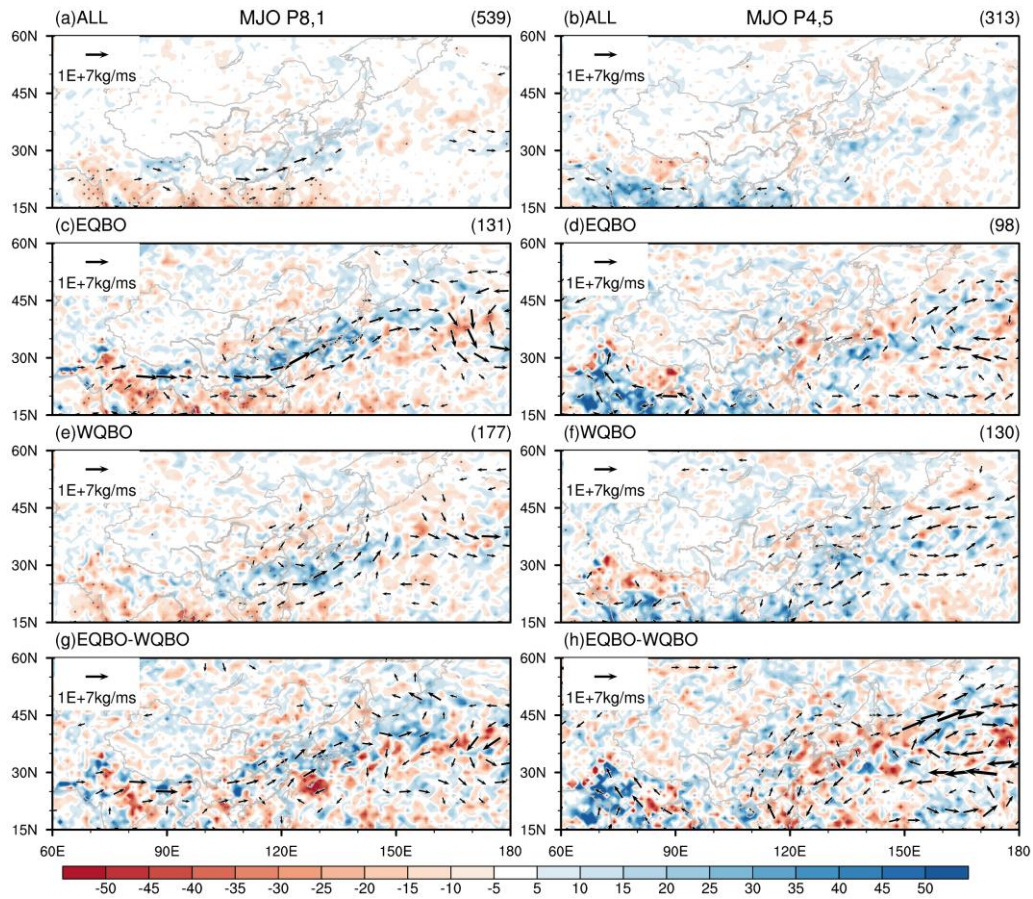
Figure S19. Composited vertically integrated moisture flux (VIMF) anomalies (vectors; units: 10^7 kg m^{-1} s^{-1}) and the VIMF horizontal convergence (VIMFC) anomalies (shadings; units: kg m^{-2} s^{-1}) using the ERA5 reanalysis during the MJO phases (left) 8-1 and (right) phases 4-5 for (a, b) total days, (c, d) easterly QBO days, (e, f) westerly QBO days and (g, h) EQBO-WQBO difference. Note that only the VIMF anomalies lager than 0.5×10^7 kg m^{-1}s^{-1} are shown. The VIMFC anomalies that are statistically significant at the 95% confidence level are dotted.